

Stellar photometry with Multi Conjugate Adaptive Optics

Giuliana Fiorentino^a, Davide Massari^{a,b}, Alan McConnachie^c, Peter B. Stetson^c, Giuseppe Bono^{d,e}, Paolo Turri^{c,f}, David Andersen^c, Jean-Pierre Veran^c, Emiliano Diolaiti^a, Laura Schreiber^a, Paolo Ciliegi^a, Michele Bellazzini^a, Eline Tolstoy^b, Matteo Monelli^g, Giacinto Iannicola^e, Ivan Ferraro^e, and Vincenzo Testa^e

^aINAF-Osservatorio Astronomico di Bologna, via Ranzani 1, 40127, Bologna, Italy

^bUniversity of Groningen, Kapteyn Astronomical Institute, NL-9747 AD Groningen, The Netherlands

^cHerzberg Astronomy and Astrophysics, National Research Council Canada, 5071 West Saanich Road, Victoria, BC V9E 2E7, Canada

^dDipartimento di Fisica, Università di Roma Tor Vergata, Via della Ricerca Scientifica 1, 00133 Roma, Italy

^eINAF-Osservatorio Astronomico di Roma, Via Frascati 33, 00040 Monte Porzio Catone, Italy

^fDepartment of Physics and Astronomy, University of Victoria, 3800 Finnerty Road, Victoria, BC V8P 5C2, Canada

^gInstituto de Astrofísica de Canarias, Calle Via Lactea s/n, E38205 La Laguna, Tenerife, Spain.

ABSTRACT

We overview the current status of photometric analyses of images collected with Multi Conjugate Adaptive Optics (MCAO) at 8-10m class telescopes that operated, or are operating, on sky. Particular attention will be paid to resolved stellar population studies. Stars in crowded stellar systems, such as globular clusters or in nearby galaxies, are ideal test-particles to test AO performance. We will focus the discussion on photometric precision and accuracy reached nowadays. We briefly describe our project on stellar photometry and astrometry of Galactic globular clusters using images taken with GeMS at the Gemini South telescope. We also present the photometry performed with DAOPHOT suite of programs into the crowded regions of these globulars reaching very faint limiting magnitudes $K_s \sim 21.5$ mag on moderately large fields of view (~ 1.5 arcmin squared). We highlight the need for new algorithms to improve the modeling of the complex variation of the Point Spread Function (PSF) across the field of view. Finally, we outline the role that large samples of stellar standards plays in providing a detailed description of the MCAO performance and in precise and accurate colour-magnitude diagrams.

Keywords: Photometry, Adaptive Optics, Resolved Stellar Populations, Globular Clusters

1. INTRODUCTION

Resolved stellar populations are crucial diagnostics to improve our understanding of the early formation and evolution of giant and dwarf galaxies in the Local Group. The Local Group is an unique laboratory to constrain cosmological simulations. The current cold dark matter model predicts that large galaxies like Andromeda and the Milky Way assembled at early epochs from merging of several dwarf galaxies. Solid constraints on the early formation and evolution of giant galaxies rely on deep and accurate color magnitude diagrams (CMDs), covering optical and near infrared (NIR) bands, and on updated stellar evolutionary models (¹).

These investigations are going to be extend out to the Local Universe in the near future thanks to the extremely large telescopes equipped with sophisticated Adaptive Optics (AO) systems. These new observing facilities will allow us to explore in detail the stellar content of elliptical galaxies, a morphological type that is

Further author information: (Send correspondence to G.F.)

: E-mail: giuliana.fiorentino@oabo.inaf.it, Telephone: +39 051 2095318

not present among Local galaxies. We need to reach a very high spatial resolution, at the diffraction limit of 30-m class telescope, to resolve into stars the extremely crowded regions of these galaxies located at distances of ~ 20 Mpc (Fornax, Virgo galaxy cluster). In the last few years we are contributing with detailed scientific cases to shape the technological requirements that will allow us to accomplish the quoted scientific goals. NFIRAOS⁽²⁾ and MAORY^(3,4) will be the first light AO modules that will assist the Thirty Meter Telescope (TMT) and the European Extremely Large Telescope (E-ELT) respectively. The Multi Conjugate Adaptive Optics (MCAO) modules available in these facilities will assure spatial resolution at the diffraction limit for a quite large FoV (a few arcmin) when compared with Single Conjugate AO (SCAO, tens of arcsec) modules. This will allow us to increase stellar statistics across the FoV, a key ingredient in resolved stellar population studies of nearby galaxies. Paving the way for extremely large telescopes means to carry out: *i)* systematic and detailed analyses of the performance expected by the MCAO modules in combination with high resolution cameras (e.g., MAORY+MICADO⁵ system); *ii)* a comprehensive investigation of the photometric and astrometric performance of AO facilities currently operating at 8–10m class telescopes. Resolved stellar populations in Galactic stellar clusters are the optimal benchmark to constrain these new observing facilities. They host thousands of stars extending several arcmin on the sky, thus sampling the full scientific FoV and they naturally provide several cluster bright stars to be used as natural guide stars (NGS) for the tip-tilt correction.

A significant fraction of the 23 nights (2007–2008) that were offered for *science demonstration* of the Multi-conjugate Adaptive optics Demonstrator mounted at the VLT (MAD@VLT⁶) were mainly dedicated to stellar clusters^(7–19) plus a few exceptions^(20,21). MAD (pixel scale of 0.028 arcsec/pix) demonstrated the capability to correct the atmospheric turbulence effect reaching almost the diffraction limit on a large FoV of ~ 2 arcmin. Although, MAD was built using “*leftovers from previous ESO (AO) projects*”⁽²²⁾, it has been a successful experiment and provided front-end science as clearly presented in the review paper by Melnick, Marchetti and Amico⁽²²⁾. For this reason, in 2009, the scientific community was quite disappointed in learning that MAD was not going to be offered anymore. The choice of stellar clusters as targets was mainly driven by the opportunity to easily identify three bright ($R \lesssim 13.5$ mag) NGS, within a circle of 2 arcmin of diameter, i.e., the asterism for MAD real time correction. It is worth mentioning that the issue of finding “bright” and ideal asterisms of NGS is an open problem for both SCAO and MCAO and will only partially be solved by future all-sky surveys (e.g. Gaia). This problem will be further enhanced when ELTs will become available, e.g., the limiting magnitude for NGS in MAORY is $H \sim 22$ mag. Future ground-based optical (LSST) and space NIR (WFIRST, EUCLID) surveys are going to alleviate these limitations. Melnick, Marchetti and Amico 2012⁽²²⁾ summarized the top-level scientific requirements for a MCAO imager, they are: *i)* stable and uniform PSF in a large FoV; *ii)* accurate photometry with a large dynamic range; *iii)* high astrometric precision, all three at or near the diffraction limit of the telescope. MAD satisfied most of them, but there was still room for improvements in terms of PSF stability with time⁽¹⁶⁾ and in terms of astrometric precision (a factor of two larger than expected¹⁸). The take home message from the MAD experiment was that classical photometric packages (like DAOPHOT²³) work well with MCAO images as soon as the PSF is uniform. Indeed, they usually prefer uniform image quality to non uniform, but high-strehl ratio images.

The use of laser guide stars provided by the Gemini Multi-conjugate adaptive optics System (GeMS) operating at the Gemini South telescope^(24,25) telescope was expected, and succeeded, to offer a much higher spatial uniformity and time stability for an almost diffraction limited PSF (in K_s -band) across the ~ 2 arcmin FoV. GeMS (pixel scale of 0.02 arcsec/pix) is the only MCAO module working with both laser (five) and natural (three) guide stars, thus resembling MAORY in its MCAO mode (six laser plus three NGS). GeMS requires three NGS with magnitude $R \lesssim 15.5$ mag, thus increasing the MAD sky-coverage. GeMS technical performance in terms of Strehl ratio and Full Width High Maximum reached across the FoV, their dependence on the wavelength are summarized in Tables 1 and 2 of⁽²⁶⁾. GeMS is routinely operating at the Gemini South and it already has had a strong impact on science^(26–34).

During the last few years, we have collected data of crowded Galactic globular clusters (GCs) using the most sophisticated AO modules operating on sky, including FLAO@LBT⁽³⁵⁾, MAD@VLT, GeMS@Gemini. We plan to collect more data using new planned AO facilities, such as LUCI-FLAO@LBT, Linc-NIRVANA@LBT, ERIS@VLT and HAWK-I-AOF@VLT. Our systematic study is demonstrating that the exploitation of AO data is far from being trivial due to the variation of the PSF across the FoV and to its time-variability that either

hamper or limit the co-adding of scientific frames to increase the overall Signal to Noise ratio. Nevertheless, these data allowed us to estimate the absolute ages of GCs with an unprecedented accuracy (a factor of two smaller than classical methods,^{12,31,36,37} see Section 2.1). Moreover, the use of GeMS and HST images for NGC 6681 allowed us to test the astrometric performance that can be reached by GeMS highlighting the importance of accounting for geometric distortion⁽³⁸⁾. In particular, we have shown that it is possible to reach a precision of ~ 0.4 mas in measuring the position of stars with multi epoch observations, in good agreement with similar investigations.³⁹ Furthermore, we have derived for the first time proper motions using GeMS anchored to HST images obtaining a precision of 0.43 mas yr^{-1} and an accuracy of 0.03 mas yr^{-1} (Massari et al. 2016d, submitted). These errors are similar to those based only on HST images, thus supporting current capabilities to pave the road for future developments in AO technology.

2. THE SCIENTIFIC FRAMEWORK: THE AGE OF THE UNIVERSE AND THE HUBBLE CONSTANT H_0

Cosmological results based on recent Cosmic microwave background (CMB) experiments (Boomerang, WMAP, PLANCK), on Baryonic Acoustic oscillations (BAO⁴⁰), on supernovae observations^(41,42) and on gravitational lensing⁽⁴³⁾ opened the path to the era of precision cosmology. However, the quoted experiments are affected by an intrinsic degeneracy in the estimate of cosmological parameters, and in particular, for the Hubble constant H_0 . To overcome this problem either specific priors or the results of different experiments are used⁽⁴⁴⁾.

Recent evaluations of the H_0 based on CMB provide values ranging from $70.0 \pm 2.2 \text{ km s}^{-1} \text{ Mpc}^{-1}$ (WMAP⁴⁵) to $67.8 \pm 0.9 \text{ km s}^{-1} \text{ Mpc}^{-1}$ ⁽⁴⁶⁾. Similar values have also been obtained by BAO plus supernovae using the so-called inverse distance ladder suggesting a value of $68.6 \pm 2.2 \text{ km s}^{-1} \text{ Mpc}^{-1}$ ⁽⁴⁷⁾. On the other hand, resolved objects (Cepheids plus supernovae) provide H_0 values ranging from 73 ± 2 (random) ± 4 (systematic) $\text{km s}^{-1} \text{ Mpc}^{-1}$ ⁽⁴⁸⁾ to $73.00 \pm 1.75 \text{ km s}^{-1} \text{ Mpc}^{-1}$ ⁽⁴¹⁾. Slightly larger values of the Hubble constant were obtained by using gravitational lens time delays ($80.0^{+4.5}_{-4.7} \text{ km s}^{-1} \text{ Mpc}^{-1}$ uniform H_0 in flat ΛCDM ⁴³).

The range of Hubble constant values indicates that there is some tension between the results based on CMB and BAO and those based on primary and secondary distance indicators. This implies an uncertainty on the age of the universe $-t_0-$ of the order of 2 Gyr. Thus having a substantial impact not only on galaxy formation and evolution, but also on the age of the GCs.

It is worth mentioning that we are also facing a stark disagreement concerning the early formation of the Galactic halo. Using a sizable sample of GCs (~ 60) observed with ACS at HST, it has been suggested that they do obey to two different age-metallicity relations⁽⁴⁹⁾. Their working hypothesis is that GCs of the metal-rich branch were formed in the disk (red solid line in Fig. 1), while those belonging to the metal-poor one were accreted into the Halo (blue solid line in Fig. 1). Oddly enough, a previous study using a very similar dataset suggested that only a subsample of GCs do obey to an age-metallicity relation whereas the bulk of them seems to be coeval ($\sim 12.8 \text{ Gyr} \pm 5\%$ ⁵⁰). This suggests that the first sample was accreted from metal-poor dwarf galaxies (blue solid line in Fig. 1) while the coeval GCs were formed in situ (grey region in Fig. 1). This evidence indicates that current absolute age estimates of GCs are affected by theoretical, empirical and intrinsic uncertainties:

Theoretical– Stellar evolutionary models adopted to construct cluster isochrones are affected by uncertainties in the physical inputs. In particular, in the adopted micro (opacity, equation of state, astrophysical screening factors) and in macro-physics (mixing length, mass loss, atomic diffusion, radiative levitation, color-temperature transformations). The impact that the quoted ingredients have on cluster isochrones have been discussed in detail in the literature⁽⁵¹⁾. The typical uncertainty in the adopted clock –the main sequence Turn Off (MSTO)– is of the order of a few percent. Thus suggesting that theoretical uncertainties does not appear to be the dominant source in the error budget of the absolute age of GCs.

Empirical– The main source of uncertainty in the absolute age estimate of GCs are the individual distances ($\Delta\mu_0 \sim 0.1 \text{ mag}$ in the true distance modulus implies an uncertainty of more than 1 Gyr in the absolute age).

Intrinsic– Dating back to more than forty years ago, spectroscopic investigations brought forward a significant star-to-star variation in C and in N among cluster stars⁽⁵²⁾. This evidence was soundly complemented by variation in Na, Al, and in O and by anti-correlations in CN-CH and in O-Na and Mg-Al⁽⁵³⁾.

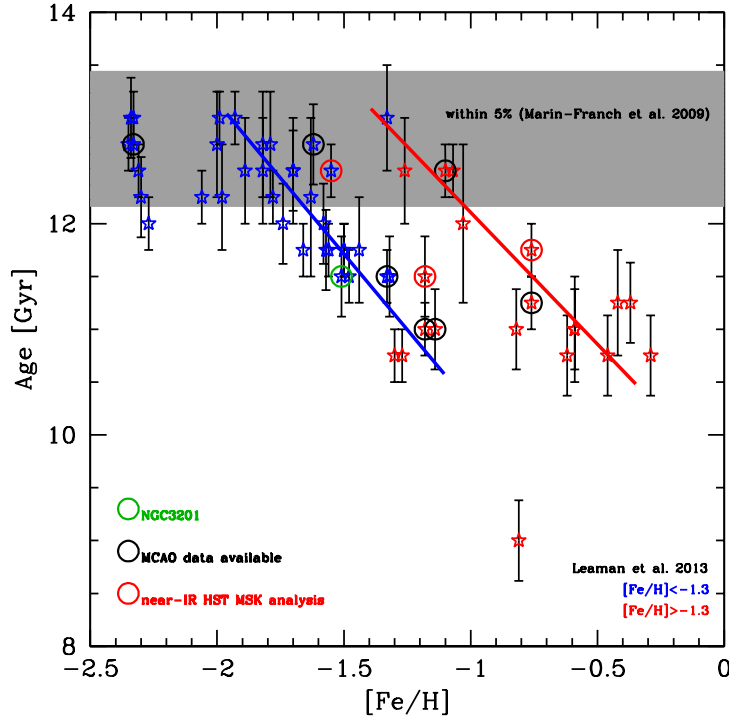


Figure 1. Age–metallicity diagram for GCs for which HST photometry is available together with the analysis of their relative ages. Data are taken from Leaman et al. 2013.⁴⁹ With red and blue stars we have highlighted the cluster metallicity, i.e., metal-rich and metal-poor, respectively. Circles indicate the clusters for which deep MCAO (black) and HST (red) NIR data are available for the MSK characterization. Blue and red lines display the two age–metallicity relations,⁴⁹ while the grey region shows the result found by Marin-Franch et al. 2009,⁵⁰ see text for more details.

The above evidence has further strengthened by the occurrence of multiple stellar populations in more massive clusters.^{54, 55} However, detailed investigations concerning the different stellar populations indicate a difference in age that is, in canonical GCs, on average shorter than 1 Gyr.⁵⁶ The intrinsic uncertainty does not seem to be the main source of the error budget of the GCs absolute age. To overcome the quoted uncertainties, different approaches have been suggested mainly based on relative age estimates, the so-called vertical and horizontal methods (^{50, 51}).

In this context the relative age is estimated as a difference between the clock (Main Sequence Turn Off, MSTO) and an evolved reference point either the horizontal branch (HB) or a specific point along the red giant branch. The key advantage of these methods is that they are independent of uncertainties on cluster distance and reddening. However, they rely on the assumption that the reference points are independent of cluster age and introduce new theoretical uncertainties (conductive opacities, extra-deep mixing along the RGB). It goes without saying that the transformation from relative to absolute ages using a reference GC introduces the typical uncertainties already discussed. In the following we describe a new method introduced by Bono and collaborators (¹²) and based mainly on deep NIR photometry.

2.1 Absolute ages of Globular clusters and the Main Sequence Knee–method

The Main Sequence Knee has been observed using NIR observations in several Galactic stellar systems, mainly globular^{12, 30, 31, 55, 57–62} and old open clusters,⁶³ in the bulge.⁶⁴ Although, this feature has been detected and characterized in optical bands,^{36, 37} it can be easily identified in the NIR regime. In cold (effective temperatures less than $\sim 4000\text{K}$) and low mass stars ($\sim 0.5 M_{\odot}$), the opacity in the stellar atmosphere starts to be dominated by the collisional induced absorption (CIA) of transitional dipole state in molecules such as $\text{H}_2\text{--H}_2$, $\text{H}_2\text{--He}$,

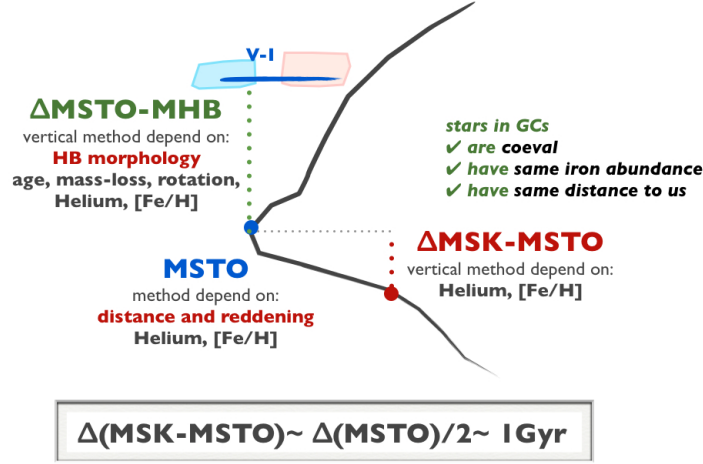


Figure 2. Cartoon representing the MSTO point in the CMD and the two vertical methods that anchor the MSTO to different evolved, the Horizontal Branch (darkgreen dotted vertical line), and un-evolved, the Main Sequence Knee (red dotted vertical line) evolutionary features. The dependencies affecting the different methods to derive absolute ages are also depicted in the Figure together with the improvement on the age accuracy when using the Main Sequence Knee.

N_2-N_2 , CH_4-CH_4 .^{65–67} The CIA mechanism acts as an absorber for wavelengths larger than $1.0 \mu m$ and an emitter in UV-visible light, thus causing a bluer main sequence for low mass stars. This means that a strong change in the main sequence slope can be observed at longer wavelengths, i.e., the Main Sequence Knee (MSK), see Fig. 2.

Using MCAO images from MAD of the GC NGC 3201,¹² suggested a new diagnostic based on the change in slope of the low main sequence as a precise age-indicator*. The advantage of using this new vertical anchor when compared to other more popular features in the CMD, such as the HB, is its negligible age dependence. The HB instead does depend not only on the age but also on other unknown parameters, i.e. mass loss, chemical composition, rotation and everything is shaping the complex morphology of the HB.⁶⁸ However, in order to reach the NIR MSK ($K_s \gtrsim 20$ mag) in the core of GCs from the ground we need to build deep, precise and accurate CMDs.

Since the first estimate of the absolute age of NGC 3201,¹² several authors applied this vertical method for aging a total of seven GCs (NGC 6838–M 71;³⁶ M 15–NGC 7078;³⁷ NGC 2808;³¹ 47 Tuc, M 4–NGC 6121, NGC 2808 and NGC 6752⁶²). A careful analysis of the systematic and random errors to be included in the Δ MSTO–MSK method has been provided by (^{31,62}).

2.2 Space motions and stellar populations with GeMS

Our project is executed on Canadian time (PI A. McConnachie). We have collected GSAOI data assisted with GeMS for seven Galactic GCs. They are listed in Table 1 and are highlighted in Fig. 1 as black circles. The selection criteria adopted are the following: *i*) they are close enough to allow us the detection of the MSK ($d_\odot \lesssim 12$ Kpc); *ii*) they suffer small amount of reddening ($E(B-V) \lesssim 0.25$); *iii*) they cover a large range in metallicity, thus providing a good sample to calibrate the MSK method as a function of the metal content ($-2.4 \lesssim [Fe/H] \lesssim -0.8$); *iv*) they have deep HST images that can be used as first epoch for deriving proper motions; *v*) they span several Kpc in Galactocentric distance ($2 \text{ Kpc} \lesssim d_G \lesssim 16 \text{ Kpc}$).

*Details on the actual point used to define the MSK is fully described in¹² and³¹ and it is the flex point before the change of curvature of the low main sequence.

Table 1. Properties of selected GCs for GeMS observations. NOTE: ^a age from Leaman et al. 2013 (⁴⁹).

GC's name	$\langle[\text{Fe}/\text{H}]\rangle$	age ^a $\pm \sigma_{age}$ Gyr	d_G Kpc	M_V mag
NGC1851	-1.18	11.00 ± 0.25	16.6	-8.33
NGC2808	-1.14	11.00 ± 0.38	11.1	-9.39
NGC5904(M5)	-1.33	11.50 ± 0.25	6.2	-8.81
NGC6681(M70)	-1.62	12.75 ± 0.38	2.2	-7.12
NGC7078(M15)	-2.33	12.75 ± 0.25	10.4	-9.19
NGC6723	-1.10	12.50 ± 0.25	2.6	-7.83
NGC6652	-0.76	11.25 ± 0.25	2.7	-6.66

Our sample (and in particular the age of NGC 6652), when fully analysed, will provide solid constraints on the two proposed Galactic halo formation scenarios (Fig. 1,^{49,50}). So far we have carefully analysed data for NGC 1851 (^{30,61}) and NGC2808 (³¹) and we have obtained accurate and precise CMDs reaching $K_s \sim 21.5$ mag, thus well below the MSK point. However, firm conclusions require more data of metal-rich GCs belonging to the *young* branch (age smaller than 11.5 Gyr, see Fig. 1): i.e., NGC 5927, NGC 6304, NGC 6352, NGC 6366, NGC 6496, NGC 6624, NGC 6637 (M 69) and Pal 12. Among the more metal-rich GCs, the MSK method has been applied to 47Tuc⁶² and M 71³⁶ and it returns age values compatible within one σ to that obtained by Vandenberg and collaborators (^{49,51}), i.e., 11.75 vs 11.6 Gyr and 11.00 vs 12.00 Gyr, respectively. For NGC 6652, the data are already in hand but we need Flamingos-2 calibration data (accepted with priority B) in order to complete our analysis.

3. THE IMPACT OF PRECISE AND ACCURATE PHOTOMETRY ON RESOLVED STELLAR POPULATIONS

The difference between photometric precision and accuracy can be synthesized in our ability to repeat photometric measurements around a specific mean value (with a small dispersion) and in our ability to measure the *true* magnitude of a star. We discuss more in detail the impact that these two concepts have on the construction of CMDs. In a precise and accurate CMD we require evolutionary sequences to appear well defined within a few hundredths of a magnitude. Once properly modeled these CMDs allow us a complete characterization of the global properties of the stellar system, and in the understanding of their formation and evolution (¹). Photometric precision and accuracy are tightly coupled issues in dealing with ground-based and space observations. The former issue is mainly related to how well we model the PSF across the scientific FoV; special attention is paid to crowded stellar environments (such as cores of GCs). The latter issue is linked to our knowledge of the observing facility (optics plus camera) and on the availability of a sizable sample of local stellar standards within the scientific FoV. The absolute photometric calibration might include several ingredients: magnitude and color terms, atmospheric-extinction and spatial dependence.

When dealing with AO observations (and in particular with SCAO), the complexity in modeling the spatial variation of the PSF and the limited FoV (small sample of calibrating stars) makes more difficult the effort to obtain accurate and precise CMDs. The former problem can be mitigated whenever a large number of bright and isolated sources are present in the field and a detailed approach in modeling the PSF is followed (^{16,69,70}). Using the NIR images collected for the GC M15 with PISCES-FLAO@LBT, we found that a careful data reduction has to be performed in dealing with images from SCAO modules. This limitation becomes even more severe when exploring the core of GCs (⁷¹). We have performed photometry of these images using an updated version of ROMAFOT that offers the opportunity to model the PSF variation across the FoV with asymmetric analytical functions. The impact of asymmetric PSF on the CMD of M15 is a well defined MSTO and narrower MS, RGB and HB sequences (see Fig. 6 in⁷¹). The width in colour of the quoted evolutionary features is a solid science-based approach to quantify photometric errors. In principle photometric errors are the main cause of the broadening of the CMD features, since the underlying stellar population is almost coeval and chemically homogeneous. Furthermore, a large number of calibrating standard stars in the field is mandatory to obtain an accurate photometric calibration, and to check if residual positional effects are present, due to the variation of the PSF.

Although, in the case of MCAO the above problems are naturally alleviated, they are still worrisome. We have presented the case of NGC 1851 observed with GeMS ⁽³⁰⁾ where a fine-tuning in the PSF modeling and in the (absolute and inter-chips) calibration enabled us to disentangle the two sub-giant branches previously observed with HST in this cluster. The offset between the two sequences is $\delta_{OFFSET} \sim 0.05$ mag at $V=19$ mag. These double sub-giants may represent an age separation of ~ 1 Gyr or a chemical difference between two coexisting populations in NGC 1851.⁷² Evolutionary models, supported by detailed spectroscopic observations of Red Giant Branch stars, seem to prefer the latter hypothesis. They suggest that the bright sequence is associated to a stellar population with a normal α enhancement while the faint one to another population with an overabundance of C+N+O ⁽⁷³⁾. A more detailed discussion of the full data reduction using DAOPHOT suite of programs and several technical issues can be found in Turri et al. 2016 (this conference⁷⁴). Here, we remember that DAOPHOT describes the PSF model by the sum of a symmetric analytic bivariate function (typically a Lorentzian or Moffat) and an empirical look-up table representing corrections to this analytic function from the observed brightness values within the average profile of several bright stars in the image. The empirical look-up table makes it possible to account for the PSF variations (from linear to cubic) across the FoV. In Turri et al. 2016,⁷⁴ we show how an increase in the degree of the PSF variation across the FoV is needed in order to minimize the residuals left over by the subtraction of all the stars from GeMS images using the assumed PSF model. This is also visible by an inspection of the CMDs obtained using different assumptions on the PSF variation. Furthermore, we have also shown that the choice of the PSF radius has a strong impact on the width of the main evolutionary sequences.

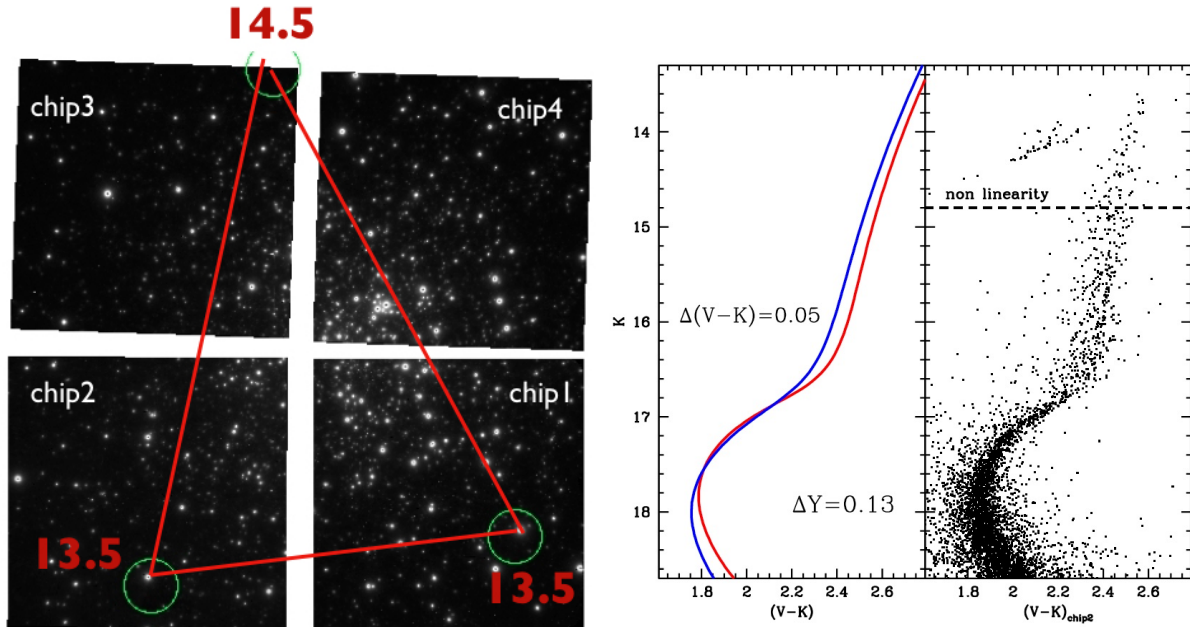


Figure 3. *Left panel*: Image for NGC2808 taken with GSAOI@GeMS. The asterism of the NGS used is highlighted together with their R-band magnitudes. *Right panels*: **sx**– Theoretical isochrones for the metallicity of NGC 2808 and for two helium abundances, primordial He ($Y=0.245$, red line) and enriched of $\Delta Y = 0.13$ (blue line); **dx**– Optical vs NIR CMD for NGC 2808 obtained using only stars located in Chip2 of GeMS images. The non linear regime has been highlighted with a dashed line.

We have performed a similar photometric analysis using GeMS data for NGC 2808 (fully described in³¹). An example of our images is shown in Fig. 3 (left panel) together with the asterism used for the NGS. This GC has the same metallicity of NGC 1851, but different HB morphology. NGC 2808 hosts several (up to five) stellar sub-populations that could be modeled with different helium abundances ($\Delta Y = 0.13$ ⁷⁵). The complexity of NGC 2808 is even enhanced by the discovery of five distinct groups of stars along the Na-O anti-correlation⁷⁶ not exactly corresponding to those identified using different helium abundances ⁽⁷⁵⁾. Fig. 3 (right-sx panel)

shows the expected maximum split in colour of the RGB due to $\Delta Y = 0.13$ is $V - K_s \sim 0.05$ mag at $K_s \sim 16$ mag. The optical–NIR CMD derived combining HST and GeMS data show a significant spread in the RGB not present in the SGB (right–dx panel). Although, we are not able to identify sub–structures in the RGB, its width in colour seems to be real. Using the images collected in eight different epochs we estimated the precision (repeatability) of our measurements that is $\sigma(K_s) \sim 0.03$ mag. Thus supporting the lack of a clear color separation among the different sub–populations. In passing we note that the combination of optical (V) and NIR (K_s) bands it is not optimal for the study of multiple helium sequences. A complex helium abundance distribution, as that suggested for NGC 2808, would require a precision smaller than 0.01 mag to be fully detected.

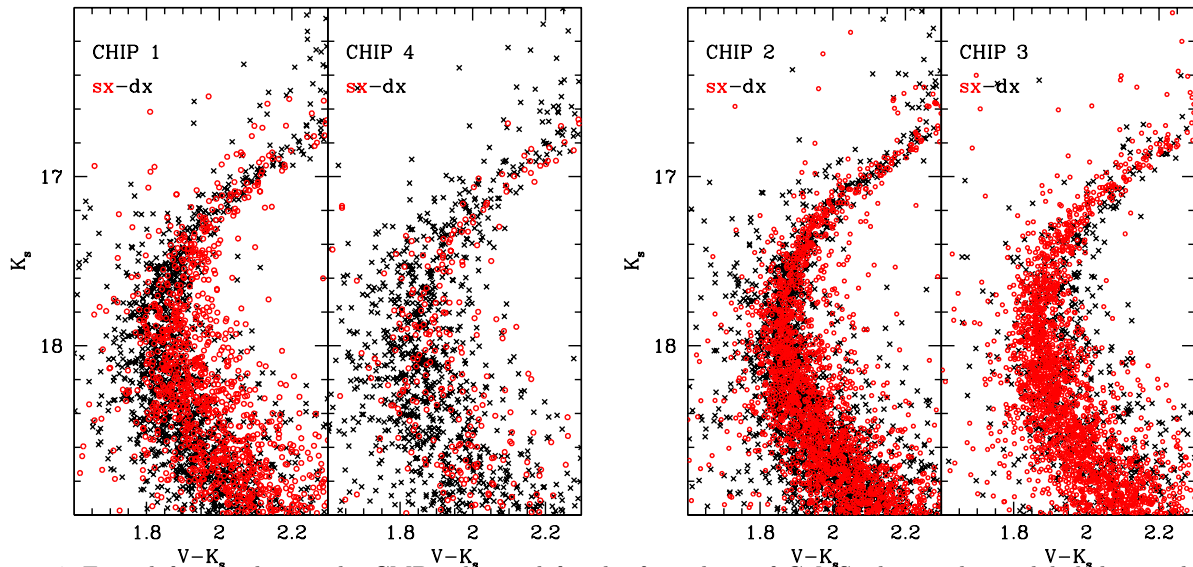


Figure 4. From left to right panels, CMDs obtained for the four chips of GeMS, the number is labeled in each panel. We have used different colour-code in order to highlight photometry coming from the left (sx, red) and right (dx, black) regions on individual chips.

We have performed the calibration onto the 2MASS photometric system by means of an intermediate catalogue derived using archival HAWK-I data for NGC 2808. Mounted at UT–4, HAWK-I camera has the advantage to have a large FoV ($\sim 7.5 \times 7.5$ arcmin) and a small pixel scale (0.106 arcsec/pixel). Thus it offers the maximum overlap with both the deep diffraction limited GeMS data ($14 \text{ mag} \lesssim K \lesssim 21.5 \text{ mag}$) and the shallow 2MASS seeing–limited data ($K \lesssim 14 \text{ mag}$), thus improving the final photometric accuracy. We have selected a range of about 2 magnitudes ($15 \text{ mag} \lesssim K \lesssim 17 \text{ mag}$) that do not suffer non–linearity in order to make a reliable calibration of each GeMS chip to HAWK-I data. Although, we have applied only zero points (no trend with magnitudes and colours was found) and we have used the same approach in calibrating the four chips, the final result does not seem satisfactory neither for the inter–chips calibration³¹ nor for the existence of spatial trend within each individual chip, as shown in Fig. 4. We have divided the single–chip photometry in two catalogues along the x–axis. Stars on the left side of the chip (sx–stars) are indicated with red open circles and those on the right side (dx) with black crosses. By an inspection of this figure, it is clear that the mean position of the MSTO show a clear x–axis trend in three chips out of four. The only exception is Chip 2. This may depend on the major uniformity of the MCAO correction, i.e., the FWHM is ~ 0.08 across the full Chip 2 as shown in Fig. 1 (left panel) of Massari et al. 2016 (³¹). This allows us a better modeling of the PSF across the Chip 2. Only the photometry of Chip 2 was used for the estimation of the absolute cluster age with the MSK method.

Although, seeing–limited data strongly suffer of blending effect (⁷⁴), we can use them to test the spatial dependency of our photometry across the FoV, see Fig. 5. In this figure differences between GeMS and HAWK-I magnitudes for calibrating stars are shown as a function of X and Y axes for both J and K bands. The linear fit for the stars are also shown (black solid lines), their slopes range from 0.0002–0.002 for the J–band and from –0.001–0.004 for the K–band in the X–direction and from –0.0006–0.003 for the J–band and from –0.0002–0.002

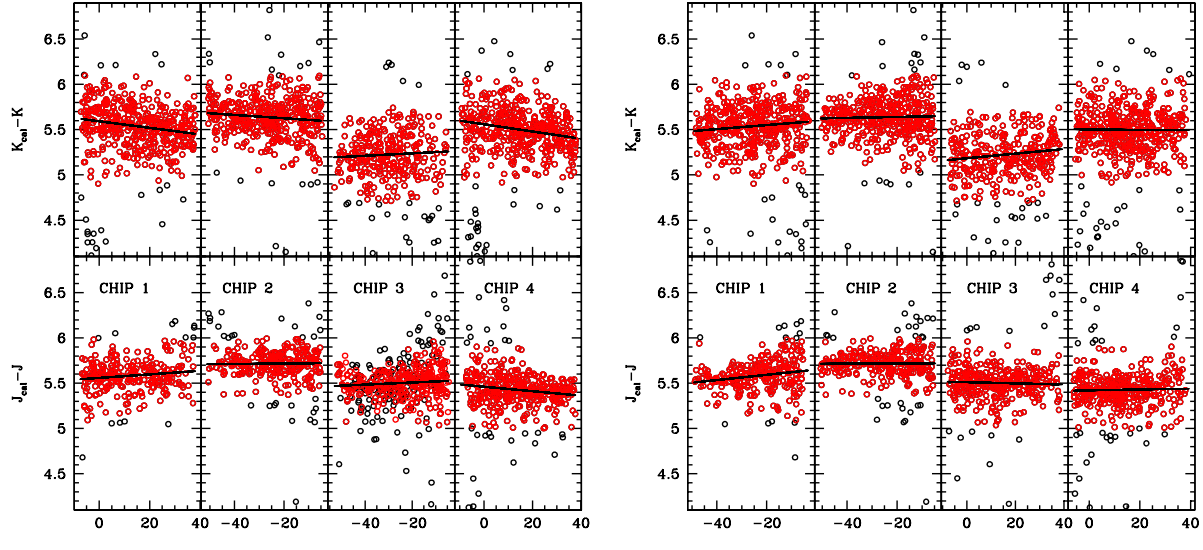


Figure 5. *Left panel:* From the left to the right Chip 1 to Chip 4. X-axis spatial distribution of the difference in magnitude between GeMS and HAWK-I calibrating stars (red open circles) in both K and J filters. Black solid lines show the linear fit. *Right panel:* Same the left panel for the Y-axis.

for the K-band in the Y-direction. Chip 2 again shows the smallest spatial dependence when compared with the others, even though the slope of the K-band in the X-direction is not zero (-0.0018) we neglected the correction because the magnitude difference distribution shows a large scatter ($\sigma/N_{stars} \sim 0.01$ mag). In a forthcoming investigation we plan to better model this spatial variation in order to use the photometry of the four chips to build a precise and accurate CMD of NGC 2808.

3.1 Numerical experiments on crowding and photometric errors

In order to quantify photometric errors in the constructed CMDs, one of the most popular approach is to perform an artificial star test. This method consists in adding a certain number of artificial stars of known magnitude (injected synthetic stars) to real images and then in extracting their magnitudes by performing once again the photometry (see for more details^{1,77}). This step is fundamental in the comparison between observations and theory, and in turn in the correct interpretation of the CMD. DAOPHOT suite of programs has a sub-routine (ADDSTAR algorithm²³) to inject artificial stars given a grid of magnitudes and positions. The comparison between injected and retrieved stellar magnitudes allow us to quantify the completeness and the photometric errors for each bin of magnitude. The full procedure is based on the assumption that we have a good model of the PSF that can allow us to add stars in real images. This is a solid assumption for space-based observations for which we have an accurate knowledge of the final PSF, since it is stable in space and in time. However, this is not the case for ground-based images, in particular, for those taken with AO-modules. As a matter of fact, the results of this test are expected to be strongly related to our ability in modeling the PSF across the FoV. This is the reason why artificial star tests have rarely been applied to AO-images. The most popular approach to quantify the photometric completeness of images collected with AO-modules has been the use of deep HST photometry (^{16,31}).

Here we present a simplified test for one image in K_s -band of the GC NGC 2808. K_s band is expected to have the largest spatial dependence as shown in Fig. 5. In particular, we focus our attention on the two chips showing the smallest (Chip 2) and the largest (Chip 1) spatial colour variation along the X-direction (see Fig. 4). The PSF was modeled using DAOPHOT: *i*) we selected ~ 100 – 200 bright and isolated stars uniformly distributed across the FoV; *ii*) we fit their brightness profile with an analytic function plus a look-up table of the residuals that vary across the FoV with a cubic dependence on the position; *iii*) we injected stars with instrumental magnitudes ranging from $K_s \sim 9$ to 14 mag accordingly to this PSF model. This interval corresponds to calibrated K_s magnitudes from ~ 14.5 to 19.5 mag.

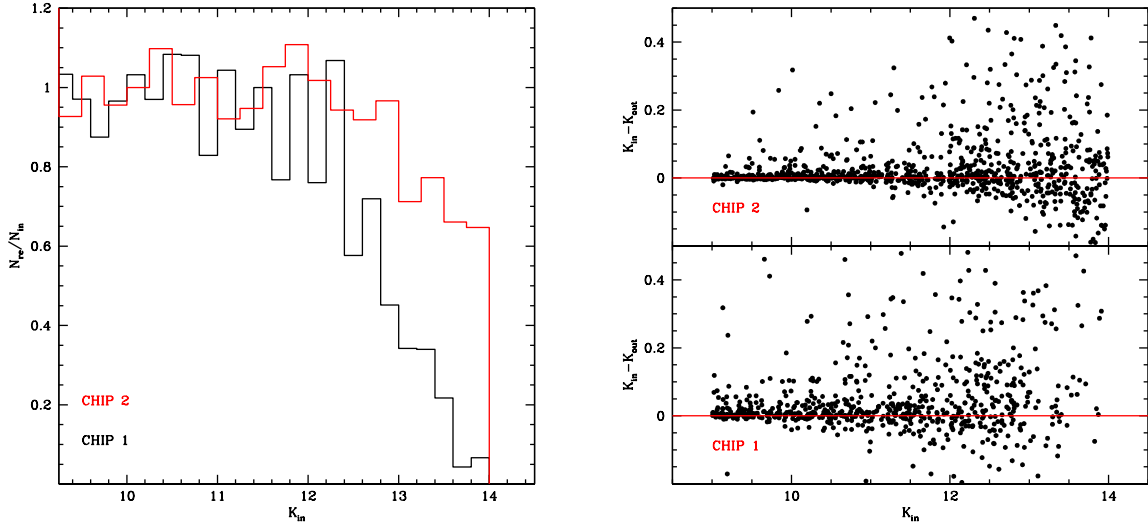


Figure 6. *Left panel:* The ratio between the number of retrieved and injected stars when performing an artificial star test. The same ratio is also called completeness. This test was applied to one K_s -band image of NGC 2808: chips 1 and 2. *Right panel:* Difference in magnitude between injected and retrieved stars adopted for the artificial star test.

Fig. 6 (left panel) shows that the completeness is dropping down very rapidly in Chip 1 when compared with Chip2, similarly to what found using HST photometry (see Fig. 5 of³¹). Moreover, the photometric errors (Fig. 6, right panel) also show a relevant decrease in the MCAO performance between the two chips. The difference $K_{in} - K_{out}$ is less than ~ 0.01 mag down to ~ 12 mag and to ~ 14 mag in Chips 1 and 2, respectively. The dispersion around the mean value of the magnitude difference is also a good approximation of the photometric error⁽⁷⁸⁾. It typically ranges—when moving from bright ($K_s \sim 9$ mag) to faint ($K_s \sim 14$ mag)—from 0.03 to ~ 0.15 mag for Chip 1 and from 0.005 to ~ 0.1 mag for Chip 2.

Finally, we investigated the behaviour of the magnitude difference between injected and retrieved stars as a function of the X and the Y-direction, (see Fig 7). A glance at the content of this figure reveals that there is no trend with the position of the stars, this applies to both Chip 1 and Chip 2. However, we have already discussed in the previous section that real seeing limited stars—observed with HAWK-I at VLT—display a well defined radial trend in the X-direction of Chip 1. This evidence seems to suggest that a classical artificial star test applied to AO-images may underestimate photometric errors when a variation of the PSF across the FoV can not be neglected. This is the consequence of the poor a-priori knowledge of *true PSF* model, since we are forced to use the *extracted PSF* to inject stars into the real image. This notwithstanding the artificial star test seems to be appropriate to quantify the degree of completeness of the stellar populations and to estimate how the crowding affects the photometry.

4. SUMMARY AND CONCLUSIONS

During the last few years we are experimenting a new class of AO facilities at the 8–10 m class telescopes, e.g., MAD@VLT, MAD@VLT, GeMS@Gemini, PISCES and LUCI-FLAO@LBT, Linc-NIRVANA@LBT, ERIS and HAWK-I-AOF@VLT. In this investigation we have focussed our attention to MCAO systems that provide a quite uniform correction on a moderately large FoV (a few arcmin). These features are ideal to study in detail resolved stellar populations in the Milky Way (GCs, Galactic bulge, Nuclear Bulge) and in nearby galaxies. Detailed resolved stellar population studies allow us also to characterize the astrometric and photometric performance of these sophisticated AO systems. This is a nowadays stepping stone to fully exploit the unprecedented observing facilities of near future ELTs.

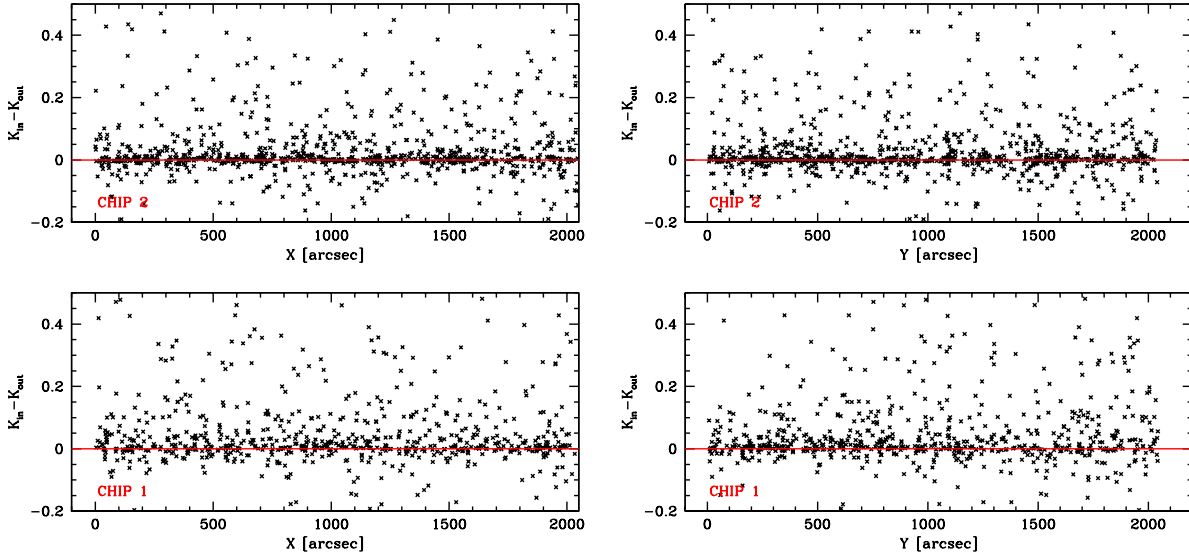


Figure 7. Spatial variation along the X (left) and the Y (right) direction of the injected and retrieved magnitudes for the artificial star test of Chip 1 (bottom panels) and Chip 2 (top panels).

We have focussed our attention on data taken with GeMS@Gemini–South telescope for some Galactic GCs. They have been already presented in a series of papers (^{30,31,61,74} Massari et al., 2016, A&A, submitted). We have carefully analysed these images reaching a limiting magnitude in $K_s \sim 21.5$ mag and the main scientific outcomes are the following: *i*) disentangle the two populations showing up along the SGB of NGC 1851 and detect the MSK; *ii*) accurate and precise estimate of the absolute age of NGC 2808, $t=10.9\pm0.7$ (intrinsic) ±0.45 (metallicity term) Gyr, in good agreement with previous studies; *iii*) to derive precise (0.43 mas yr^{-1}) and accurate (0.03 mas yr^{-1}) proper motions for NGC 6681 using HST data as first epoch and GeMS as second epoch.

The overall scientific analyses show that the quality of GeMS data is enough to reach astrometric and photometric precisions similar to that of HST in optical bands. In this investigation we also outline the main issues when dealing with AO images and the need for a new genuine approach. The leading steps in this novel approach are the following:

PSF modeling: Although, MCAO corrects a quite large FoV and provide an almost uniform diffracted limited PSF across the images, the residual variation of the PSF can not be neglected and has to be carefully modeled. We have shown that standard photometric data reduction on MCAO images is feasible. However, there are still some residual effects that need to be undertaken to optimize the scientific return of these new challenging instruments. This requirement becomes even more relevant in dealing with SCAO images. In the last years, the community devoted a paramount effort in updating existing and in developing new software to accomplish data reduction of AO images: *STARFINDER*, with an hybrid modeling that allows the adaptation of the parameters of the analytical part over the FoV and also takes into account for the contribution of the numerical residuals (^{69,79}); *PATCH*, a software developed for image restoration with spatially variable PSF (⁸⁰); *ROMAFOT* with an analytical PSF model that varies across the FoV and account also for asymmetric components (^{71,81}). It is worth to mention that information coming from PSF–reconstruction techniques⁸² can provide a robust ingredient for these update versions of photometric data reduction codes.

Complex calibration: To obtain accurate and precise CMDs we need a careful absolute calibration. All sky NIR survey performed by 2MASS was a quantum jump in photometric accuracy, since it opened a new and solid approach to calibrate NIR photometry. However, it is too shallow ($K \lesssim 14, H \lesssim 15, J \lesssim 15.8$ mag) and the spatial resolution (~ 0.5 arcsec) inadequate for crowded stellar fields. Indeed the large pixel scale makes difficult to

select not blended stars in 2MASS catalogues and faint 2MASS stars are typically saturated in images collected with 8–10m class telescopes assisted with AO. An intermediate step is necessary and a possible strategy might be the pre-AO-imaging with similar 8–10m telescopes, but either in seeing limited conditions (e.g., Flamingos-2 at Gemini South) or enhanced by GLAO systems (e.g., HAWK-I at VLT). Once again the smaller FoV offered by SCAO systems makes these issues even more complex when compared with MCAO images. As extensively discussed here, the opportunity to have at disposal such intermediate catalogues allow us to investigate in detail the technical performance of AO-systems. These NIR calibrating stars will also be crucial in the future to select the NGS and in turn the optimal asterism for ELTs.

ACKNOWLEDGMENTS

Based on published results obtained using MAD at the VLT and on proprietary observations obtained at the Gemini Observatory and acquired through the Gemini Science Archive. GF and DM has been supported by the FIRB 2013 (MIUR grant RBFR13J716). GF thanks the SPIE organizers for this invited paper and B. Neichel and G. Sivo for the useful discussion during this 2016 SPIE conference in Edinburgh.

REFERENCES

- [1] Gallart, C., Aparicio, A., and Vilchez, J. M., “The Local Group Dwarf Irregular Galaxy NGC 6822.I.The Stellar Content,” *AJ* **112**, 1928–+ (Nov. 1996).
- [2] Herriot, G., Andersen, D., Atwood, J., Boyer, C., Byrnes, P., Caputa, K., Ellerbroek, B., Gilles, L., Hill, A., Ljusic, Z., Pazder, J., Rosensteiner, M., Smith, M., Spano, P., Szeto, K., Véran, J.-P., Wevers, I., Wang, L., and Wooff, R., “NFIRAOS: first facility AO system for the Thirty Meter Telescope,” in [*Adaptive Optics Systems IV*], *Proc. SPIE* **9148**, 914810 (July 2014).
- [3] Diolaiti, E., Conan, J.-M., Foppiani, I., Marchetti, E., Baruffolo, A., Bellazzini, M., Bregoli, G., Butler, C. R., Ciliegi, P., Cosentino, G., Delabre, B., Lombini, M., Petit, C., Robert, C., Rossettini, P., Schreiber, L., Tomelleri, R., Biliotti, V., D’Odorico, S., Fusco, T., Hubin, N., and Meimon, S., “Conceptual design and performance of the multiconjugate adaptive optics module for the European Extremely Large Telescope,” in [*Society of Photo-Optical Instrumentation Engineers (SPIE) Conference Series*], *Society of Photo-Optical Instrumentation Engineers (SPIE) Conference Series* **7736** (July 2010).
- [4] Diolaiti, E., t. M. c., “MAORY: adaptive optics module for the E-ELT,” in [*This SPIE conference*], *This SPIE conference* (2016).
- [5] Davies, R., Ageorges, N., Barl, L., Bedin, L. R., Bender, R., Bernardi, P., Chapron, F., Clenet, Y., Deep, A., Deul, E., Drost, M., Eisenhauer, F., Falomo, R., Fiorentino, G., Förster Schreiber, N. M., Gendron, E., Genzel, R., Gratadour, D., Greggio, L., Grupp, F., Held, E., Herbst, T., Hess, H.-J., Hubert, Z., Jahnke, K., Kuijken, K., Lutz, D., Magrin, D., Muschielok, B., Navarro, R., Noyola, E., Paumard, T., Piotto, G., Ragazzoni, R., Renzini, A., Rousset, G., Rix, H.-W., Saglia, R., Tacconi, L., Thiel, M., Tolstoy, E., Trippe, S., Tromp, N., Valentijn, E. A., Verdoes Kleijn, G., and Wegner, M., “MICADO: the E-ELT adaptive optics imaging camera,” in [*Society of Photo-Optical Instrumentation Engineers (SPIE) Conference Series*], *Society of Photo-Optical Instrumentation Engineers (SPIE) Conference Series* **7735** (July 2010).
- [6] Marchetti, E., Brast, R., Delabre, B., Donaldson, R., Fedrigo, E., Frank, C., Hubin, N., Kolb, J., Lizon, J.-L., Marchesi, M., Oberti, S., Reiss, R., Soenke, C., Tordo, S., Baruffolo, A., Bagnara, P., Amorim, A., and Lima, J., “MAD on sky results in star oriented mode,” in [*Society of Photo-Optical Instrumentation Engineers (SPIE) Conference Series*], *Society of Photo-Optical Instrumentation Engineers (SPIE) Conference Series* **7015** (July 2008).
- [7] Bouy, H., Kolb, J., Marchetti, E., Martín, E. L., Huélamo, N., and Barrado Y Navascués, D., “Multi-conjugate adaptive optics images of the Trapezium cluster,” *A&A* **477**, 681–690 (Jan. 2008).
- [8] Gullieuszik, M., Greggio, L., Held, E. V., Moretti, A., Arcidiacono, C., Bagnara, P., Baruffolo, A., Diolaiti, E., Falomo, R., Farinato, J., Lombini, M., Ragazzoni, R., Brast, R., Donaldson, R., Kolb, J., Marchetti, E., and Tordo, S., “Resolving stellar populations outside the Local Group: MAD observations of UKS 2323-326,” *A&A* **483**, L5–L8 (May 2008).

- [9] Bouy, H., Huélamo, N., Martín, E. L., Marchis, F., Barrado Y Navascués, D., Kolb, J., Marchetti, E., Petr-Gotzens, M. G., Sterzik, M., Ivanov, V. D., Köhler, R., and Nürnberger, D., “A deep look into the cores of young clusters. I. σ -Orionis,” *A&A* **493**, 931–946 (Jan. 2009).
- [10] Ferraro, F. R., Dalessandro, E., Mucciarelli, A., Beccari, G., Rich, R. M., Origlia, L., Lanzoni, B., Rood, R. T., Valenti, E., Bellazzini, M., Ransom, S. M., and Cocozza, G., “The cluster Terzan 5 as a remnant of a primordial building block of the Galactic bulge,” *Nature* **462**, 483–486 (Nov. 2009).
- [11] Moretti, A., Piotto, G., Arcidiacono, C., Milone, A. P., Ragazzoni, R., Falomo, R., Farinato, J., Bedin, L. R., Anderson, J., Sarajedini, A., Baruffolo, A., Diolaiti, E., Lombini, M., Brast, R., Donaldson, R., Kolb, J., Marchetti, E., and Tordo, S., “MCAO near-IR photometry of the globular cluster NGC 6388: MAD observations in crowded fields,” *A&A* **493**, 539–546 (Jan. 2009).
- [12] Bono, G., Stetson, P. B., VandenBerg, D. A., Calamida, A., Dall’Ora, M., Iannicola, G., Amico, P., Di Cecco, A., Marchetti, E., Monelli, M., Sanna, N., Walker, A. R., Zoccali, M., Buonanno, R., Caputo, F., Corsi, C. E., Degl’Innocenti, S., D’Odorico, S., Ferraro, L., Gilmozzi, R., Melnick, J., Nonino, M., Ortolani, S., Piersimoni, A. M., Prada Moroni, P. G., Pulone, L., Romaniello, M., and Storm, J., “On a New Near-Infrared Method to Estimate the Absolute Ages of Star Clusters: NGC 3201 as a First Test Case,” *ApJL* **708**, L74–L79 (Jan. 2010).
- [13] Campbell, M. A., Evans, C. J., Mackey, A. D., Gieles, M., Alves, J., Ascenso, J., Bastian, N., and Longmore, A. J., “VLT-MAD observations of the core of 30 Doradus,” *MNRAS* **405**, 421–435 (June 2010).
- [14] Crowther, P. A., Schnurr, O., Hirschi, R., Yusof, N., Parker, R. J., Goodwin, S. P., and Kassim, H. A., “The R136 star cluster hosts several stars whose individual masses greatly exceed the accepted $150M_{\text{stellar}}$ mass limit,” *MNRAS* **408**, 731–751 (Oct. 2010).
- [15] Sana, H., Momany, Y., Gieles, M., Carraro, G., Beletsky, Y., Ivanov, V. D., de Silva, G., and James, G., “A MAD view of Trumpler 14,” *A&A* **515**, A26 (June 2010).
- [16] Fiorentino, G., Tolstoy, E., Diolaiti, E., Valenti, E., Cignoni, M., and Mackey, A. D., “MAD about the Large Magellanic Cloud. Preparing for the era of Extremely Large Telescopes,” *A&A* **535**, A63 (Nov. 2011).
- [17] Ortolani, S., Barbuy, B., Momany, Y., Saviane, I., Bica, E., Jilkova, L., Salerno, G. M., and Jungwiert, B., “A Fossil Bulge Globular Cluster Revealed by very Large Telescope Multi-conjugate Adaptive Optics,” *ApJ* **737**, 31 (Aug. 2011).
- [18] Meyer, E., Kürster, M., Arcidiacono, C., Ragazzoni, R., and Rix, H.-W., “Astrometry with the MCAO instrument MAD. An analysis of single-epoch data obtained in the layer-oriented mode,” *A&A* **532**, A16 (Aug. 2011).
- [19] Rochau, B., Brandner, W., Stolte, A., Henning, T., Da Rio, N., Gennaro, M., Hormuth, F., Marchetti, E., and Amico, P., “A benchmark for multiconjugated adaptive optics: VLT-MAD observations of the young massive cluster Trumpler 14,” *MNRAS* **418**, 949–959 (Dec. 2011).
- [20] Mignani, R. P., Falomo, R., Moretti, A., Treves, A., Turolla, R., Sartore, N., Zane, S., Arcidiacono, C., Lombini, M., Farinato, J., Baruffolo, A., Ragazzoni, R., and Marchetti, E., “Near infrared VLT/MAD observations of the isolated neutron stars RX J0420.0-5022 and RX J1856.5-3754,” *A&A* **488**, 267–270 (Sept. 2008).
- [21] Falomo, R., Pian, E., Treves, A., Giovannini, G., Venturi, T., Moretti, A., Arcidiacono, C., Farinato, J., Ragazzoni, R., Diolaiti, E., Lombini, M., Tavecchio, F., Brast, R., Donaldson, R., Kolb, J., Marchetti, E., and Tordo, S., “The jet of the BL Lacertae object PKS 0521-365 in the near-IR: MAD adaptive optics observations,” *A&A* **501**, 907–914 (July 2009).
- [22] Melnick, J., Marchetti, E., and Amico, P., “Science with ESO’s Multi-conjugate Adaptive-optics Demonstrator - MAD,” in [*Adaptive Optics Systems III*], *Proc. SPIE* **8447**, 84470M (July 2012).
- [23] Stetson, P. B., “The center of the core-cusp globular cluster M15: CFHT and HST Observations, ALL-FRAME reductions,” *PASP* **106**, 250–280 (Mar. 1994).
- [24] Rigaut, F., Neichel, B., Boccas, M., d’Orgeville, C., Arriagada, G., Fesquet, V., Diggs, S. J., Marchant, C., Gausach, G., Rambold, W. N., Luhrs, J., Walker, S., Carrasco-Damele, E. R., Edwards, M. L., Pessev, P., Galvez, R. L., Vucina, T. B., Araya, C., Gutierrez, A., Ebbers, A. W., Serio, A., Moreno, C., Urrutia, C., Rogers, R., Rojas, R., Trujillo, C., Miller, B., Simons, D. A., Lopez, A., Montes, V., Diaz, H., Daruich, F., Colazo, F., Bec, M., Trancho, G., Sheehan, M., McGregor, P., Young, P. J., Doolan, M. C., van Harmelen,

- J., Ellerbroek, B. L., Gratadour, D., and Garcia-Rissmann, A., “GeMS: first on-sky results,” in [*Adaptive Optics Systems III*], *Proc. SPIE* **8447**, 84470I (July 2012).
- [25] Rigaut, F., Neichel, B., Boccas, M., d’Orgeville, C., Vidal, F., van Dam, M. A., Arriagada, G., Fesquet, V., Galvez, R. L., Gausachs, G., Cavedoni, C., Ebberts, A. W., Karewicz, S., James, E., Lührs, J., Montes, V., Perez, G., Rambold, W. N., Rojas, R., Walker, S., Bec, M., Tranco, G., Sheehan, M., Irarrazaval, B., Boyer, C., Ellerbroek, B. L., Flicker, R., Gratadour, D., Garcia-Rissmann, A., and Daruich, F., “Gemini multiconjugate adaptive optics system review - I. Design, trade-offs and integration,” *MNRAS* **437**, 2361–2375 (Jan. 2014).
- [26] Neichel, B., Vidal, F., Rigaut, F., Rodrigo Carrasco, E., Arriagada, G., Serio, A., Pessev, P., Winge, C., van Dam, M., Garrel, V., Araujo, C., Boccas, M., Fesquet, V., Galvez, R., Gausachs, G., Lührs, J., Montes, V., Moreno, C., Rambold, W., Trujillo, C., Urrutia, C., and Vucina, T., “Gems first science results,” *ArXiv e-prints* (Jan. 2014).
- [27] Davidge, T. J., “GeMS in the Outer Galaxy: Near-infrared Imaging of Three Young Clusters at Large Galactic Radii,” *ApJ* **781**, 95 (Feb. 2014).
- [28] Saracino, S., Dalessandro, E., Ferraro, F. R., Lanzoni, B., Geisler, D., Mauro, F., Villanova, S., Moni Bidin, C., Miocchi, P., and Massari, D., “GEMINI/GeMS Observations Unveil the Structure of the Heavily Obscured Globular Cluster Liller 1,” *ApJ* **806**, 152 (June 2015).
- [29] Manchado, A., Stanghellini, L., Villaver, E., García-Segura, G., Shaw, R. A., and García-Hernández, D. A., “High-resolution Imaging of NGC 2346 with GSAOI/GeMS: Disentangling the Planetary Nebula Molecular Structure to Understand Its Origin and Evolution,” *ApJ* **808**, 115 (Aug. 2015).
- [30] Turri, P., McConnachie, A. W., Stetson, P. B., Fiorentino, G., Andersen, D. R., Véran, J.-P., and Bono, G., “Toward Precision Photometry for the ELT Era: The Double Subgiant Branch of NGC 1851 Observed with the Gemini/GeMS MCAO System,” *ApJL* **811**, L15 (Oct. 2015).
- [31] Massari, D., Fiorentino, G., McConnachie, A., Bono, G., Dall’Ora, M., Ferraro, I., Iannicola, G., Stetson, P. B., Turri, P., and Tolstoy, E., “GeMS MCAO observations of the Galactic globular cluster NGC 2808: the absolute age,” *A&A* **586**, A51 (Feb. 2016).
- [32] Santos, Jr., J. F. C., Roman-Lopes, A., Carrasco, E. R., Maia, F. F. S., and Neichel, B., “GeMS/GSAOI observations of La Serena 94: an old and far open cluster inside the solar circle,” *MNRAS* **456**, 2126–2139 (Feb. 2016).
- [33] Opitz, D., Tinney, C. G., Faherty, J. K., Sweet, S., Gelino, C. R., and Kirkpatrick, J. D., “Searching for Binary Y Dwarfs with the Gemini Multi-conjugate Adaptive Optics System (GeMS),” *ApJ* **819**, 17 (Mar. 2016).
- [34] Bernard, A., Neichel, B., Samal, M. R., Zavagno, A., Andersen, M., Evans, C. J., Plana, H., and Fusco, T., “Deep GeMS/GSAOI near-infrared observations of N159W in the Large Magellanic Cloud,” *ArXiv e-prints* (May 2016).
- [35] Esposito, S., Riccardi, A., Pinna, E., Puglisi, A. T., Quirós-Pacheco, F., Arcidiacono, C., Xompero, M., Briguglio, R., Busoni, L., Fini, L., Argomedo, J., Gherardi, A., Agapito, G., Brusa, G., Miller, D. L., Guerra Ramon, J. C., Boutsia, K., and Stefanini, P., “Natural guide star adaptive optics systems at LBT: FLAO commissioning and science operations status,” in [*Adaptive Optics Systems III*], *Proc. SPIE* **8447**, 84470U (July 2012).
- [36] Di Cecco, A., Bono, G., Prada Moroni, P. G., Tognelli, E., Allard, F., Stetson, P. B., Buonanno, R., Ferraro, I., Iannicola, G., Monelli, M., Nonino, M., and Pulone, L., “On the Absolute Age of the Metal-rich Globular M71 (NGC 6838). I. Optical Photometry,” *AJ* **150**, 51 (Aug. 2015).
- [37] Monelli, M., Testa, V., Bono, G., Ferraro, I., Iannicola, G., Fiorentino, G., Arcidiacono, C., Massari, D., Boutsia, K., Briguglio, R., Busoni, L., Carini, R., Close, L., Cresci, G., Esposito, S., Fini, L., Fumana, M., Guerra, J. C., Hill, J., Kulesa, C., Mannucci, F., McCarthy, D., Pinna, E., Puglisi, A., Quiros-Pacheco, F., Ragazzoni, R., Riccardi, A., Skemer, A., and Xompero, M., “The Absolute Age of the Globular Cluster M15 Using Near-infrared Adaptive Optics Images from PISCES/LBT,” *ApJ* **812**, 25 (Oct. 2015).
- [38] Massari, D., Fiorentino, G., Tolstoy, E., McConnachie, A., Stuik, R., Schreiber, L., Andersen, D., Clénet, Y., Davies, R., Gratadour, D., Kuijken, K., Navarro, R., Pott, J.-U., Rodeghiero, G., Turri, P., and Verdoes Kleijn, G., “High-precision astrometry towards ELTs,” *ArXiv e-prints* (July 2016).

- [39] Neichel, B., Lu, J. R., Rigaut, F., Ammons, S. M., Carrasco, E. R., and Lassalle, E., “Astrometric performance of the Gemini multiconjugate adaptive optics system in crowded fields,” *MNRAS* **445**, 500–514 (Nov. 2014).
- [40] Eisenstein, D. J., Zehavi, I., Hogg, D. W., Scoccimarro, R., Blanton, M. R., Nichol, R. C., Scranton, R., Seo, H.-J., Tegmark, M., Zheng, Z., Anderson, S. F., Annis, J., Bahcall, N., Brinkmann, J., Burles, S., Castander, F. J., Connolly, A., Csabai, I., Doi, M., Fukugita, M., Frieman, J. A., Glazebrook, K., Gunn, J. E., Hendry, J. S., Hennessy, G., Ivezić, Z., Kent, S., Knapp, G. R., Lin, H., Loh, Y.-S., Lupton, R. H., Margon, B., McKay, T. A., Meiksin, A., Munn, J. A., Pope, A., Richmond, M. W., Schlegel, D., Schneider, D. P., Shimasaku, K., Stoughton, C., Strauss, M. A., SubbaRao, M., Szalay, A. S., Szapudi, I., Tucker, D. L., Yanny, B., and York, D. G., “Detection of the Baryon Acoustic Peak in the Large-Scale Correlation Function of SDSS Luminous Red Galaxies,” *ApJ* **633**, 560–574 (Nov. 2005).
- [41] Riess, A. G., Macri, L. M., Hoffmann, S. L., Scolnic, D., Casertano, S., Filippenko, A. V., Tucker, B. E., Reid, M. J., Jones, D. O., Silverman, J. M., Chornock, R., Challis, P., Yuan, W., Brown, P. J., and Foley, R. J., “A 2.4% Determination of the Local Value of the Hubble Constant,” *ArXiv e-prints* (Apr. 2016).
- [42] Riess, A. G., Macri, L., Casertano, S., Lampeitl, H., Ferguson, H. C., Filippenko, A. V., Jha, S. W., Li, W., and Chornock, R., “A 3% Solution: Determination of the Hubble Constant with the Hubble Space Telescope and Wide Field Camera 3,” *ApJ* **730**, 119 (Apr. 2011).
- [43] Suyu, S. H., Auger, M. W., Hilbert, S., Marshall, P. J., Tewes, M., Treu, T., Fassnacht, C. D., Koopmans, L. V. E., Sluse, D., Blandford, R. D., Courbin, F., and Meylan, G., “Two Accurate Time-delay Distances from Strong Lensing: Implications for Cosmology,” *ApJ* **766**, 70 (Apr. 2013).
- [44] Bennett, C. L., Larson, D., Weiland, J. L., and Hinshaw, G., “The 1% Concordance Hubble Constant,” *ApJ* **794**, 135 (Oct. 2014).
- [45] Hinshaw, G., Larson, D., Komatsu, E., Spergel, D. N., Bennett, C. L., Dunkley, J., Nolte, M. R., Halpern, M., Hill, R. S., Odegard, N., Page, L., Smith, K. M., Weiland, J. L., Gold, B., Jarosik, N., Kogut, A., Limon, M., Meyer, S. S., Tucker, G. S., Wollack, E., and Wright, E. L., “Nine-year Wilkinson Microwave Anisotropy Probe (WMAP) Observations: Cosmological Parameter Results,” *ApJS* **208**, 19 (Oct. 2013).
- [46] Planck Collaboration, Ade, P. A. R., Aghanim, N., Arnaud, M., Ashdown, M., Aumont, J., Baccigalupi, C., Banday, A. J., Barreiro, R. B., Battaner, E., Benabed, K., Benoit-Lévy, A., Bernard, J.-P., Bersanelli, M., Bielewicz, P., Bond, J. R., Borrill, J., Bouchet, F. R., Burigana, C., Butler, R. C., Calabrese, E., Chamballu, A., Chiang, H. C., Christensen, P. R., Clements, D. L., Colombo, L. P. L., Couchot, F., Curto, A., Cuttaia, F., Danese, L., Davies, R. D., Davis, R. J., de Bernardis, P., de Rosa, A., de Zotti, G., Delabrouille, J., Diego, J. M., Dole, H., Doré, O., Dupac, X., Enßlin, T. A., Eriksen, H. K., Fabre, O., Finelli, F., Forni, O., Frailis, M., Franceschi, E., Galeotta, S., Galli, S., Ganga, K., Giard, M., González-Nuevo, J., Górski, K. M., Gregorio, A., Gruppuso, A., Hansen, F. K., Hanson, D., Harrison, D. L., Henrot-Versillé, S., Hernández-Monteagudo, C., Herranz, D., Hildebrandt, S. R., Hivon, E., Hobson, M., Holmes, W. A., Hornstrup, A., Hovest, W., Hufenberger, K. M., Jaffe, A. H., Jones, W. C., Keihänen, E., Keskitalo, R., Kneissl, R., Knoch, J., Kunz, M., Kurki-Suonio, H., Lamarre, J.-M., Lasenby, A., Lawrence, C. R., Leonardi, R., Lesgourgues, J., Liguori, M., Lilje, P. B., Linden-Vørnle, M., López-Caniego, M., Lubin, P. M., Macías-Pérez, J. F., Mandolesi, N., Maris, M., Martin, P. G., Martínez-González, E., Masi, S., Matarrese, S., Mazzotta, P., Meinhold, P. R., Melchiorri, A., Mendes, L., Menegoni, E., Mennella, A., Migliaccio, M., Miville-Deschênes, M.-A., Moneti, A., Montier, L., Morgante, G., Moss, A., Munshi, D., Murphy, J. A., Naselsky, P., Nati, F., Natoli, P., Nørgaard-Nielsen, H. U., Noviello, F., Novikov, D., Novikov, I., Oxborrow, C. A., Pagano, L., Pajot, F., Paoletti, D., Pasian, F., Patanchon, G., Perdereau, O., Perotto, L., Perrotta, F., Piacentini, F., Piat, M., Pierpaoli, E., Pietrobon, D., Plaszczyński, S., Pointecouteau, E., Polenta, G., Ponthieu, N., Popa, L., Pratt, G. W., Prunet, S., Rachen, J. P., Rebolo, R., Reinecke, M., Remazeilles, M., Renault, C., Ricciardi, S., Ristorcelli, I., Rocha, G., Roudier, G., Rusholme, B., Sandri, M., Savini, G., Scott, D., Spencer, L. D., Stolyarov, V., Sudiwala, R., Sutton, D., Suur-Uski, A.-S., Sygnet, J.-F., Tauber, J. A., Tavagnacco, D., Terenzi, L., Toffolatti, L., Tomasi, M., Tristram, M., Tucci, M., Uzan, J.-P., Valenziano, L., Valiviita, J., Van Tent, B., Vielva, P., Villa, F., Wade, L. A., Yvon, D., Zacchei, A., and Zonca, A., “Planck intermediate results. XXIV. Constraints on variations in fundamental constants,” *A&A* **580**, A22 (Aug. 2015).

- [47] Cuesta, A. J., Vargas-Magaña, M., Beutler, F., Bolton, A. S., Brownstein, J. R., Eisenstein, D. J., Gil-Marín, H., Ho, S., McBride, C. K., Maraston, C., Padmanabhan, N., Percival, W. J., Reid, B. A., Ross, A. J., Ross, N. P., Sánchez, A. G., Schlegel, D. J., Schneider, D. P., Thomas, D., Tinker, J., Tojeiro, R., Verde, L., and White, M., “The clustering of galaxies in the SDSS-III Baryon Oscillation Spectroscopic Survey: baryon acoustic oscillations in the correlation function of LOWZ and CMASS galaxies in Data Release 12,” *MNRAS* **457**, 1770–1785 (Apr. 2016).
- [48] Freedman, W. L. and Madore, B. F., “The Hubble Constant,” *ARA&A* **48**, 673–710 (Sept. 2010).
- [49] Leaman, R., VandenBerg, D. A., and Mendel, J. T., “The bifurcated age-metallicity relation of Milky Way globular clusters and its implications for the accretion history of the galaxy,” *MNRAS* **436**, 122–135 (Nov. 2013).
- [50] Marín-Franch, A., Aparicio, A., Piotto, G., Rosenberg, A., Chaboyer, B., Sarajedini, A., Siegel, M., Anderson, J., Bedin, L. R., Dotter, A., Hempel, M., King, I., Majewski, S., Milone, A. P., Paust, N., and Reid, I. N., “The ACS Survey of Galactic Globular Clusters. VII. Relative Ages,” *ApJ* **694**, 1498–1516 (Apr. 2009).
- [51] VandenBerg, D. A., Brogaard, K., Leaman, R., and Casagrande, L., “The Ages of 55 Globular Clusters as Determined Using an Improved ΔV^{HB} TO Method along with Color-Magnitude Diagram Constraints, and Their Implications for Broader Issues,” *ApJ* **775**, 134 (Oct. 2013).
- [52] Osborn, W. H., *Positions of Globular Cluster Stars in the Physical H-R Diagram.*, PhD thesis, Yale University. (1971).
- [53] Gratton, R. G., Carretta, E., and Bragaglia, A., “Multiple populations in globular clusters. Lessons learned from the Milky Way globular clusters,” *A&A Rev.* **20**, 50 (Feb. 2012).
- [54] Bellini, A., Piotto, G., Milone, A. P., King, I. R., Renzini, A., Cassisi, S., Anderson, J., Bedin, L. R., Nardiello, D., Pietrinferni, A., and Sarajedini, A., “The Intriguing Stellar Populations in the Globular Clusters NGC 6388 and NGC 6441,” *ApJ* **765**, 32 (Mar. 2013).
- [55] Milone, A. P., Marino, A. F., Bedin, L. R., Piotto, G., Cassisi, S., Dieball, A., Anderson, J., Jerjen, H., Asplund, M., Bellini, A., Brogaard, K., Dotter, A., Giersz, M., Heggie, D. C., Knigge, C., Rich, R. M., van den Berg, M., and Buonanno, R., “The M 4 Core Project with HST - II. Multiple stellar populations at the bottom of the main sequence,” *MNRAS* **439**, 1588–1595 (Apr. 2014).
- [56] Ventura, P., D’Antona, F., Mazzitelli, I., and Gratton, R., “Predictions for Self-Pollution in Globular Cluster Stars,” *ApJL* **550**, L65–L69 (Mar. 2001).
- [57] Pulone, L., De Marchi, G., Paresce, F., and Allard, F., “The Lower Main Sequence of ω Centauri from Deep Hubble Space Telescope NICMOS Near-Infrared Observations,” *ApJL* **492**, L41–L44 (Jan. 1998).
- [58] Pulone, L., de Marchi, G., and Paresce, F., “The mass function of M 4 from near IR and optical HST observations,” *A&A* **342**, 440–452 (Feb. 1999).
- [59] Lagioia, E. P., Milone, A. P., Stetson, P. B., Bono, G., Prada Moroni, P. G., Dall’Ora, M., Aparicio, A., Buonanno, R., Calamida, A., Ferraro, I., Gilmozzi, R., Iannicola, G., Matsunaga, N., Monelli, M., and Walker, A., “On the Kinematic Separation of Field and Cluster Stars across the Bulge Globular NGC 6528,” *ApJ* **782**, 50 (Feb. 2014).
- [60] Milone, A. P., Marino, A. F., Cassisi, S., Piotto, G., Bedin, L. R., Anderson, J., Allard, F., Aparicio, A., Bellini, A., Buonanno, R., Monelli, M., and Pietrinferni, A., “The infrared eye of the Wide-Field Camera 3 on the Hubble Space Telescope reveals multiple main sequences of very low-mass stars in NGC 2808,” *ArXiv e-prints* (June 2012).
- [61] Turri, P., McConnachie, A. W., Stetson, P. B., Fiorentino, G., Andersen, D. R., Bono, G., and Véran, J.-P., “Photometric performance of LGS MCAO with science-based metrics: first results from Gemini/GeMS observations of Galactic globular clusters,” in [*Adaptive Optics Systems IV*], *Proc. SPIE* **9148**, 91483V (Aug. 2014).
- [62] Correnti, M., Gennaro, M., Kalirai, J. S., Brown, T. M., and Calamida, A., “Constraining Globular Cluster Age Uncertainties using the IR Color–Magnitude Diagram,” *ApJ* **823**, 18 (May 2016).
- [63] Sarajedini, A., Dotter, A., and Kirkpatrick, A., “Deep 2MASS Photometry of M67 and Calibration of the Main-Sequence J - K_S Color Difference as an Age Indicator,” *ApJ* **698**, 1872–1878 (June 2009).

- [64] Zoccali, M., Cassisi, S., Frogel, J. A., Gould, A., Ortolani, S., Renzini, A., Rich, R. M., and Stephens, A. W., “The Initial Mass Function of the Galactic Bulge down to $\sim 0.15 M_{\text{solar}}$,” *ApJ* **530**, 418–428 (Feb. 2000).
- [65] Saumon, D., Bergeron, P., Lunine, J. I., Hubbard, W. B., and Burrows, A., “Cool zero-metallicity stellar atmospheres,” *ApJ* **424**, 333–344 (Mar. 1994).
- [66] Borysow, A., Jorgensen, U. G., and Zheng, C., “Model atmospheres of cool, low-metallicity stars: the importance of collision-induced absorption,” *A&A* **324**, 185–195 (Aug. 1997).
- [67] Allard, F. and Hauschildt, P. H., “Model atmospheres for M (sub)dwarf stars. 1: The base model grid,” *ApJ* **445**, 433–450 (May 1995).
- [68] Salaris, M., Cassisi, S., and Pietrinferni, A., “On the red giant branch mass loss in 47 Tucanae: Constraints from the horizontal branch morphology,” *A&A* **590**, A64 (May 2016).
- [69] Schreiber, L., Diolaiti, E., Bellazzini, M., Ciliegi, P., Foppiani, I., Greggio, L., Lanzoni, B., and Lombini, M., “Handling a highly structured and spatially variable Point Spread Function in AO images,” in [*Second International Conference on Adaptive Optics for Extremely Large Telescopes. Online at <http://ao4elt2.lesia.obspm.fr>*] http://ao4elt2.lesia.obspm.fr/Aj_id.P57], P57 (Sept. 2011).
- [70] Schreiber, L., La Camera, A., Prato, M., Diolaiti, E., constraint on the PSFS which is an upper bound derived from the Strehl ratio (SR), h. s. i. g. w. s. P. a. f. t. P.-A. s. o. t. E.-E. M. s. M., and different crowding conditions., “Point Spread Function extraction in crowded fields using blind deconvolution,” in [*Proceedings of the Third AO4ELT Conference*], Esposito, S. and Fini, L., eds. (Dec. 2013).
- [71] Fiorentino, G., Ferraro, I., Iannicola, G., Bono, G., Monelli, M., Testa, V., Arcidiacono, C., Faccini, M., Gilmozzi, R., Xompero, M., and Briguglio, R., “On the use of asymmetric PSF on NIR images of crowded stellar fields,” in [*Society of Photo-Optical Instrumentation Engineers (SPIE) Conference Series*], *Society of Photo-Optical Instrumentation Engineers (SPIE) Conference Series* **9148**, 3 (Aug. 2014).
- [72] Milone, A. P., Bedin, L. R., Piotto, G., Anderson, J., King, I. R., Sarajedini, A., Dotter, A., Chaboyer, B., Marin-Franch, A., Majewski, S., Aparicio, A., Hempel, M., Paust, N. E. Q., Reid, I. N., Rosenberg, A., and Siegel, M., “The ACS Survey of Galactic Globular Clusters. III. The Double Subgiant Branch of NGC 1851,” *ApJ* **673**, 241–250 (Jan. 2008).
- [73] Cassisi, S., Salaris, M., Pietrinferni, A., Piotto, G., Milone, A. P., Bedin, L. R., and Anderson, J., “The Double Subgiant Branch of NGC 1851: The Role of the CNO Abundance,” *ApJL* **672**, L115 (Jan. 2008).
- [74] Turri, P., McConnachie, A. W., Stetson, P. B., Andersen, D. R., Véran, J., Fiorentino, G., and Massari, D., “Photometric techniques, performance and PSF characterization of GeMS,” in [*This SPIE conference*], *This SPIE conference* (2016).
- [75] Milone, A. P., Marino, A. F., Piotto, G., Renzini, A., Bedin, L. R., Anderson, J., Cassisi, S., D’Antona, F., Bellini, A., Jerjen, H., Pietrinferni, A., and Ventura, P., “The Hubble Space Telescope UV Legacy Survey of Galactic Globular Clusters. III. A Quintuple Stellar Population in NGC 2808,” *ApJ* **808**, 51 (July 2015).
- [76] Carretta, E., “Five Groups of Red Giants with Distinct Chemical Composition in the Globular Cluster NGC 2808,” *ApJ* **810**, 148 (Sept. 2015).
- [77] Gallart, C., Aparicio, A., Bertelli, G., and Chiosi, C., “The Local Group Dwarf Irregular Galaxy NGC 6822.II. The Old and Intermediate -Age Star Formation History,” *AJ* **112**, 1950–+ (Nov. 1996).
- [78] Deep, A., Fiorentino, G., Tolstoy, E., Diolaiti, E., Bellazzini, M., Ciliegi, P., Davies, R. I., and Conan, J.-M., “An E-ELT case study: colour-magnitude diagrams of an old galaxy in the Virgo cluster,” *A&A* **531**, A151 (July 2011).
- [79] Diolaiti, E., Bendinelli, O., Bonaccini, D., Close, L., Currie, D., and Parmeggiani, G., “Analysis of isoplanatic high resolution stellar fields by the StarFinder code,” *A&AS* **147**, 335–346 (Dec. 2000).
- [80] La Camera, A., Schreiber, L., Diolaiti, E., Boccacci, P., Bertero, M., Bellazzini, M., and Ciliegi, P., “A method for space-variant deblurring with application to adaptive optics imaging in astronomy,” *A&A* **579**, A1 (July 2015).
- [81] Buonanno, R. and Iannicola, G., “Stellar photometry with big pixels,” *PASP* **101**, 294–301 (Mar. 1989).
- [82] Jolissaint, L., Ragland, S., Wizinowich, P., and Bouxin, A., “Laser guide star adaptive optics point spread function reconstruction project at W. M. Keck Observatory: preliminary on-sky results,” in [*Adaptive Optics Systems IV*], *Proc. SPIE* **9148**, 91484S (July 2014).